On the new porous silicate HPM-5

Donghui Jo,[†] Alvaro Mayoral,[‡] Suk Bong Hong,[*,†] and Miguel A. Camblor[*,¶]

†*Center for Ordered Nanoporous Materials Synthesis, Division of Environmental Science and Engineering, POSTECH, Pohang, Gyeongbuk, 37673, Korea.*

‡*Advance Microscopy Laboratory (LMA), Nanoscience Institute of Aragon (INA), University of Zaragoza, Mariano Esquillor, Edificio I+D, 50018, Zaragoza, Spain.*

¶*Instituto de Ciencia de Materiales de Madrid (ICMM), Consejo Superior de Investigaciones Científicas (CSIC), Sor Juana Inés de la Cruz 3, 28049 Madrid, Spain.*

E-mail: sbhong@postech.ac.kr; macamblor@icmm.csic.es

keywords: Zeolites; Zeolite Analogues; Silicates; Microporous Materials; Nanocrystals.

This article is dedicated to the memory of our friend Professor Claudio M. Zicovich-Wilson

Abstract

HPM-5, a porous aluminosilicate with an intricate and so far unsolved structure, has been synthesized using 1,2,3-trimethylimidazolium in hydroxide medium in the absence of fluoride anions. It consistently displays an ill-defined XRD pattern with broad and overlapped reflections and contains a large concentration of defects, as evidenced by IR and ^{29}Si MAS NMR spectroscopies. ^{1}H MAS NMR confirms the existence of highly deshielded protons (resonance at -11.6 ppm) assigned to H in relatively strong Si–O–H$\cdots$O–Si hydrogen bonds (O$\cdots$O distance $\approx$ 2.64 Å). The calcined material shows a limited microporosity (0.07–0.09 cm^{3}g^{-1}). A high resolution transmission electron microscopy study suggests HPM-5 may be far more complicated than 'standard' layered zeolites and may consist of low density layers profusely decorated by holes. The

resulting lace–like layers may be too unstable to withstand reactions characteristic of more conventional layered materials (both delamination and expansion by silylation): while the derivatives show an increase in specific surface area the layers are apparently disassembled and, at most, only ribbons remain.

Introduction

Zeolites and layered silicates may be synthesized with the aid of organic species generally called structure-directing agents (SDAs).[1] Inorganic species may also play a role in directing zeolite syntheses towards a particular structure or to structures with some particular substructure. For instance, fluoride has been proposed to direct to structures containing double-four membered rings (D4R), a subunit composed of 8 tetrahedral atoms at the vertex of a cube and bridged through O atoms close to the edges of the cube.[2,3] Fluoride tends to end occluded inside that unit and its structure-directing effect has been rationalized as increasing the ionicity of the Si-O bond, hence enhancing the flexibility of the framework and, thus, affording structures that would otherwise be too unstable.[4,5]

On the other hand, if a combination of structure-directing effects proves to be effective in crystallizing a given zeolite structure, one possible strategy in a further search for new zeolites could be to hamper one particular structure-directing effect, while allowing the rest to act. For instance, the synthesis of the D4R-containing zeolite ITW apparently needs a combination of fluoride (for the D4R unit) and an organic cation based on the charged imidazolium ring with not exceedingly large substituents (1,2,3- or 1,3,4-trimethylimidazolium, 1,3-dimethylimidazolium, 1-ethyl-2,3-dimethylimidazolium and even 2-ethyl-1,3,4-trimetylimidazolium).[5–9] The crystallization of ITW, which works best at a pure silica composition, could be frustrated by working in the absence of fluoride (to hopefully avoid D4R and hence ITW) using hydroxide instead. This would in principle require to introduce some aluminum atoms in the resulting zeolite framework for charge balance. Such a synthesis could be expected to yield either ITW with no fluoride occluded and hence with

quite a lot of Al, or, instead, a zeolite with no D4Rs. This strategy has produced both a known zeolite with a high Al content (RTH, Si/Al = 10) which we already reported in a prior paper,[10] and a new (alumino)silicate termed HPM-5. Here we report on the physicochemical properties of the latter phase.

Experimental Section

A synthesis mixture with the composition 0.3ROH : 0.05KOH : 0.01Al_2O_3 : 1.0SiO_2 : 15.0H_2O, where R is 1,2,3-trimethylimidazolium (123TMI^+), was prepared by combining aluminum hydroxide ($Al(OH)_3 \cdot H_2O$, 85%, Aldrich), tetraethylorthosilicate (TEOS, 98%, Aldrich), potassium hydroxide (KOH, 85%, Aldrich), ROH, and deionized water. The iodide salt of 123TMI^+ was prepared according to the procedures described elsewhere, and then transformed into an aqueous solution of its hydroxide form.[8] In a typical synthesis, aluminum hydroxide was mixed with an appropriate amount of water in a solution of ROH and stirred at room temperature for 1 h. After adding KOH, the resulting solution was stirred for one additional hour. To this solution, a given amount of TEOS was added and stirred at room temperature or 80 °C to remove the ethanol molecules generated by the hydrolysis of TEOS plus enough water to achieve the desired composition. The final synthesis mixture was stirred at room temperature for 1 h, charged into Teflon-lined autoclaves, and then heated under rotation (60 rpm) at 150 °C for between 7 and 24 days. The solid product was recovered by filtration or centrifugation, washed repeatedly with water, and dried overnight at room temperature. As–made HPM-5 was calcined in air at 550 °C for 8 h to remove the occluded organic cations.

Powder X-ray diffraction (XRD) patterns were recorded on a PANalytical X'Pert diffractometer or a D8 Bruker Advance diffractometer (Cu K_α radiation). Thermogravimetric (TGA) and differential thermal analyses (DTA) were performed on an SII EXSTAR 6000 thermal analyzer. The N_2 sorption experiments were carried out on a Mirae SI nanoPorosity-

XG analyzer or a Micromeritics ASAP 2010 analyzer. The IR spectra in the structural region were recorded on a Nicolet 6700 FT-IR spectrometer using the KBr pellet technique.

^{1}H and ^{13}C solution NMR measurements for 123TMI^{+} iodide were carried out in 5 mm quartz tubes using a Bruker AVANCE III 300 spectrometer. The ^{1}H NMR spectra were recorded at a frequency of 300.13 MHz with a $\pi/2$ rad pulse length of 11.0 μs and a recycle delay of 2.0 s. The ^{13}C NMR spectra were recorded at a frequency of 75.475 MHz with a $\pi/2$ rad pulse length of 10.2 μs and a recycle delay of 1.5 s. Solid-state multinuclear NMR measurements were performed on Varian Unity INOVA 600 (^{1}H) and Bruker AVANCE II 500 (^{1}H-^{13}C CP, ^{27}Al and ^{29}Si) spectrometers at spinning rates of 30.0 and 6.0 kHz, respectively. The ^{1}H MAS NMR spectra were recorded at a frequency of 599.95 MHz with a $\pi/2$ rad pulse length of 5.0 μs, a recycle delay of 5.0 s, and an acquisition of 16 pulse transients. The ^{1}H-^{13}C CP MAS NMR spectra were recorded at a frequency of 75.43 MHz with a $\pi/2$ rad pulse length of 7.0 μs, a recycle delay of 3.0 s, and an acquisition of ca. 5000 pulse transients, which was repeated with a contact time of 2.5 ms. The ^{29}Si MAS NMR spectra were recorded at a frequency of 59.59 MHz with a $\pi/2$ rad pulse length of 5.0 μs, a recycle delay of 30 s, and acquisition of ca. 5000 pulse transients. The ^{1}H, ^{13}C and ^{29}Si chemical shifts are reported relative to TMS. The ^{27}Al MAS NMR spectra were recorded at a frequency of 78.16 MHz with a $\pi/8$ rad pulse length of 1.8 μs, a recycle delay of 0.5 s, and an acquisition of ca. 1000 pulse transients. The ^{27}Al chemical shifts are referenced to an $Al(H_2O)_6{}^{3+}$ solution.

Field emission scanning electron microscopy (FE-SEM) measurements were performed on a FEI NOVA NANOSEM 230, which was also equipped with an EDAX SDD Apollo 10 system for microanalysis by energy dispersive X-ray spectroscopy (EDX). Spherical aberration (C_s) corrected Scanning Transmission Electron Microscopy (STEM) were performed in a FEI TITAN XFEG 60-300 electron microscope which was operated at 300 kV. The TEM was equipped with a CEOS corrector for the electron probe allowing a point resolution of 78 pm. Prior to observation the samples were deeply crushed using mortar and pestle and dispersed on absolute ethanol; few drops of the suspension were deposited onto a holey

carbon copper microgrids.

Delamination of HPM-5 was attempted following a reported procedure:[11] 0.50 g of the as–made material were mixed with 2.82 g of hexadecyltrimethylammonium bromide (99%, Aldrich) and 6.02 g of 1.0 M tetrapropylammonium hydroxide solution (Aldrich) in 8.91 g of water. The mixture was refluxed at 80 °C for 16 h. The swollen HPM-5 was placed in an ultrasonic bath (100 W, 42 kHz) at room temperature for 3 h, and a few drops of 1.0 M HCl solution were added to adjust the pH to < 2. The solid product was recovered by centrifugation, dried in air at room temperature and calcined at 550 °C for 6 h to remove the occluded organic species.

For the silylation of HPM-5, we followed the procedure developed by Gies et al:[12] 0.08 g of dichlorodimethylsilane (98.5%, Aldrich) was added into 30 mL of 1.0 M HCl solution, followed by the addition of 0.60 g of as–made HPM-5. After stirring for 4 h at room temperature, the sample was transferred into an autoclave and heated under rotation (60 rpm) at 180 °C for 24 h. The solid product was recovered by centrifugation, dried in air at room temperature and calcined at 500 °C for 6 h.

Results and Discussion

As–made and calcined HPM-5

HPM-5 can be obtained in a rather wide range of conditions using 123TMI$^+$ with or without a metal hydroxide, MOH with M = Li^+, Na^+, K^+, Rb^+ or $NH_4{}^+$, and for Si/Al ratios generally equal or above 15 in the synthesis mixture.[10] In fact, this material dominates the crystallization field of aluminosilicates using 123TMI$^+$ in the absence of fluoride, with only RTH competing at a high Al content (Si/Al = 10) and also MFI in a much limited extent (as a minor phase at lower Al content (Si/Al = 50) when Li^+ or no metal is used).[10] Although there may occasionally be slight differences between samples prepared in different conditions with regard to their characterization, the general features of HPM-5 are essentially

maintained. HPM-5 consistently displays an ill-defined but characteristic pattern containing very broad (fwhm $\geq 0.5°$) and severely overlapped reflections (Fig. 1, bottom). There are just a few reflections that can be discerned in the 5-45°, 2θ ($\approx$ 6.7, 7.6, 9.7, 13.0, 20.9, 24.4, 25.3 and 26.6°). Calcination at 550 °C produces significant changes in the pattern: there are fewer reflections, still very broad, a little bit less overlapped and shifted to larger angles ($\approx$ 6.8, 9.1, 10.8 and 13.4°), suggesting a contraction of the unit cell. Based on their consistent XRD patterns, and as far as we know, HPM-5 is a new silicate material.

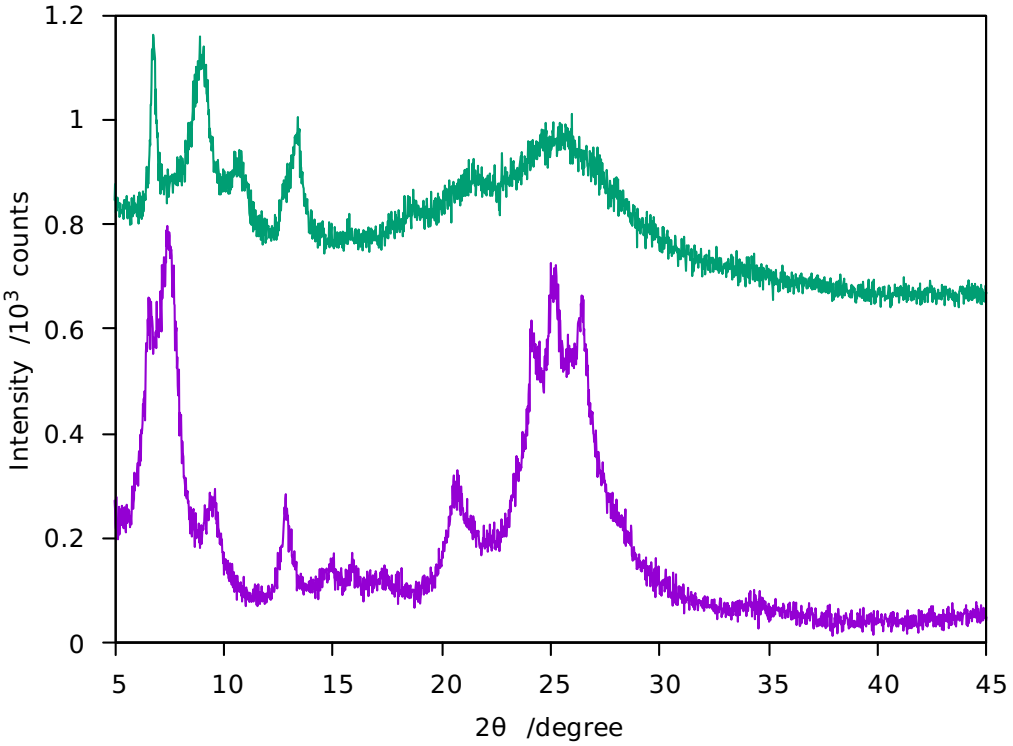

Figure 1: Powder XRD patterns of as–made (bottom) and calcined (top) forms of HPM-5 with a bulk Si/Al ratio of 30.

The IR spectra are also consistently similar among as–made HPM-5 samples. The small vibrations appearing at 1400-1600 and 680-750 cm^{-1} in the spectrum of the as–made material can be assigned to the organic cation, by comparison with the IR spectrum of pure silica ITW containing the same cation.[13] In addition to vibrational bands assigned to T-O asymmetric and symmetric stretching (1000-1300 and around 800 cm^{-1}, respectively) and to structural

subunits below 600 cm^{-1}), there is a small but clearly visible band centered around 960 cm^{-1}. This may be assigned to the Si-O vibration in Si-OH and Si-OR and suggest a significant concentration of unconnected silica tetrahedra (either structural, defective or at the surface). Interestingly, the spectrum of calcined HPM-5 still contains that band (Fig. 2, top).

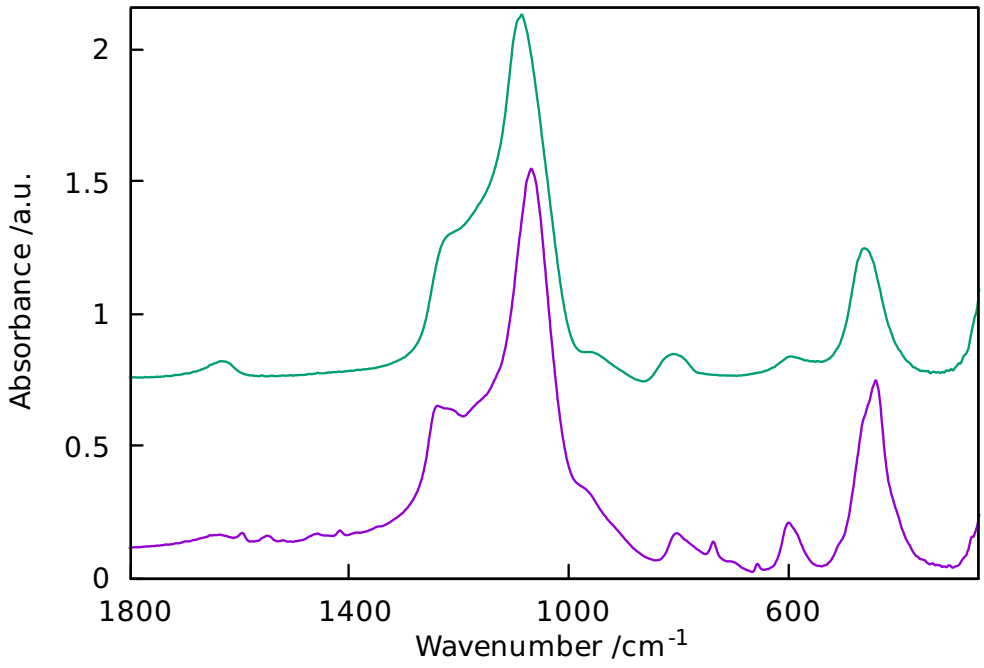

Figure 2: IR spectra of as–made (bottom) and calcined HPM-5 (top).

The FE-SEM images of as–made HPM-5 show that this material consists of particles roughly 10-40 μm wide displaying a delicate morphology that resembles carnation flowers (Fig. 3). The 'petals' are very thin (certainly smaller than 20 nm) and long (in the 5-20 μm range). While these petals seem to be rather narrow (less than 1 μm), they appear to be composed of still much narrower elements (Fig. 3, bottom). The tiny elements that compose the delicate HPM-5 flowers, which are nanosized in two dimensions, probably contributes to the existence of only broad reflections in the powder XRD pattern.

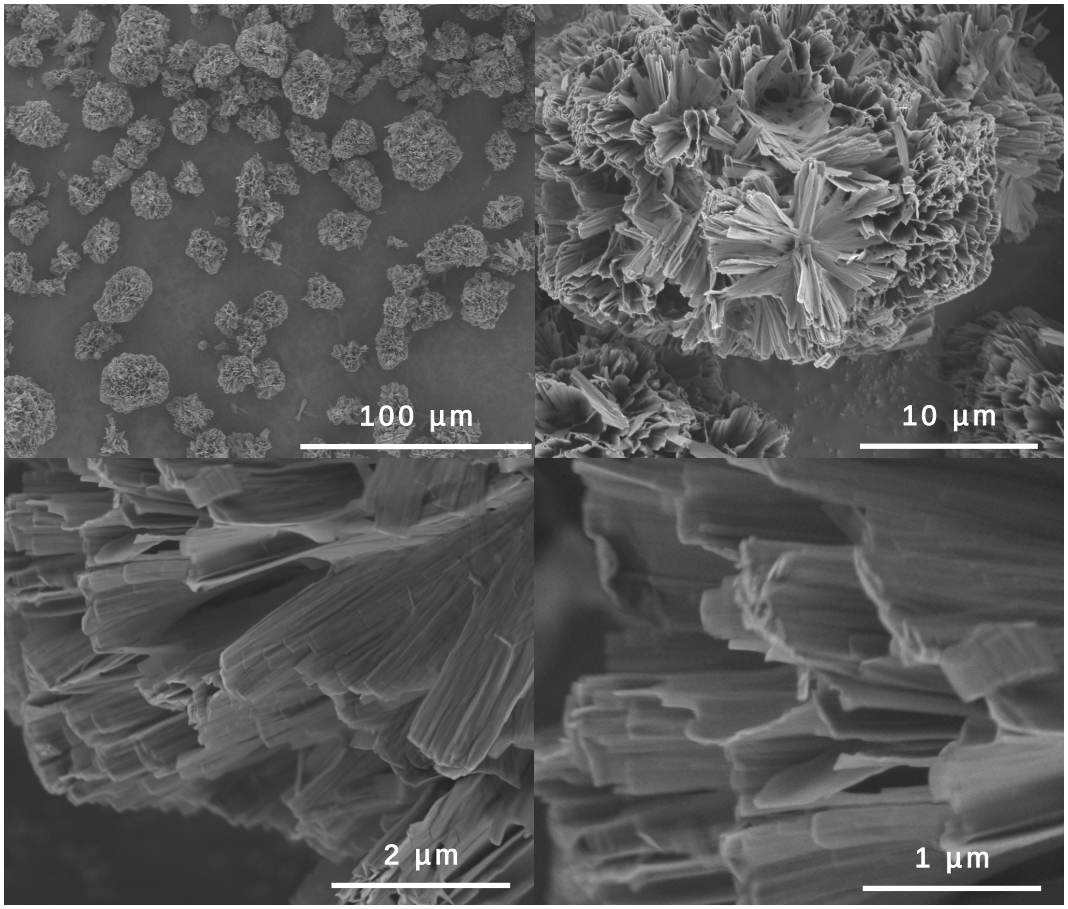

Figure 3: FE-SEM images of as–made HPM-5.

The TGA/DTA curves of as–made HPM-5 in Supporting Information Fig. S1, revealed two weight loss steps of 6.3% (from room temperature to 200 °C) and 19.6% (200–800 °C). The low temperature step mainly occurs below 120 °C and is ascribed to loosely bound physically adsorbed water. The high T step, which occurs mainly in the 250–500 °C range (almost 15%) but then extends up to 800 °C needs to be assigned to 123TMI$^+$ plus water resulting from Si–OH dehydroxilation. This is because chemical analysis (Table 1) suggests the cation is intact (the C/N ratio of 3.2 is close to the theoretical value of 3.0) but amounts merely to around 15.7% by weight, while there is a large excess hydrogen that cannot be accounted for by only the physically adsorbed water referred to above. The excess hydrogen, if due to water, amounts to 10.7% water, which is in reasonable agreement with thermal analysis: 6.3% physically adsorbed water plus 4.4% water from dehydroxilation (which,

together with 15.7% 123TMI$^+$ accounts well for the second weight step).

Table 1: Elemental and thermal analysis data of as–made HPM-5

N	C	H	C/N	H/N	excess H[a]	123TMI$^+$	H_2O_{zeo}[b]	H_2O_{SiOH}[c]
	weight%		molar ratios[d]		mol/100 g		weight%	
3.95	10.72	2.75	3.2(3.0)	9.7(5.5)	1.18	15.7	6.3	4.3

[a] H exceeding the organic content according to the N analysis, [b] Loosely bound water (low temperature step in TGA), [c] Water produced by the dehydroxilation of SiOH groups (together with 123TMI$^+$, responsible for the high temperature step in TGA), [d] Theoretical ratios for $C_6N_2H_{11}{}^+$ between parenthesis.

On the other hand, the amount of organics clearly exceeds the amount of Al in the zeolite. The chemical composition data in Table 1 correspond to a sample with a Si/Al ratio of ca. 30 (by EDX). This implies a 123TMI$^+$: Al ratio of over 3.5 : 1, thus requiring a large concentration of Si–O$^-$ groups for charge balance.

The N_2 adsorption isotherm on calcined HPM-5 in Supporting Information Fig. S2, prove the porous nature of the material. The micropore volume determined is, however, small (0.07 cm^3g^{-1}). There is a certain variability in micropore volume, which may reach up to 0.09 cm^3g^{-1} in some other samples. Similar variability in porosity depending on synthesis conditions has been reported, for instance, for MCM–35 (MTF).[14] The low micropore volume of HPM-5 somehow contrasts with its relatively large organic content. For comparison, as–made HPM-5 contains over 30% more 123TMI$^+$ than ITQ–12 (0.115 and 0.083 mol 123TMI$^+$ per mol of TO_2, respectively, where T is Si or Al) while the micropore volume of calcined ITQ–12 (0.13 $cm^3g^{\cdot 1}$)[6] is at least 40% larger than that of calcined HPM-5. This is likely due to a combination of two factors: the nanosized domains of the HPM-5 crystals, considering the known detrimental effect of the size of zeolite nanocrystals on their micropore volume,[15] and, possibly, the large structural changes associated to calcination (see Fig. 1).

The ^{1}H–^{13}C CP MAS NMR spectrum of as–made HPM-5 indicates that the organic cations are occluded intact inside the void space during the synthesis (Fig. 4, left). The ^{1}H MAS NMR spectrum (Fig. 4, right) shows three resonances assigned to the protons of the organic cations, as well as three additional resonances: a small one around 0.8 ppm (unas-

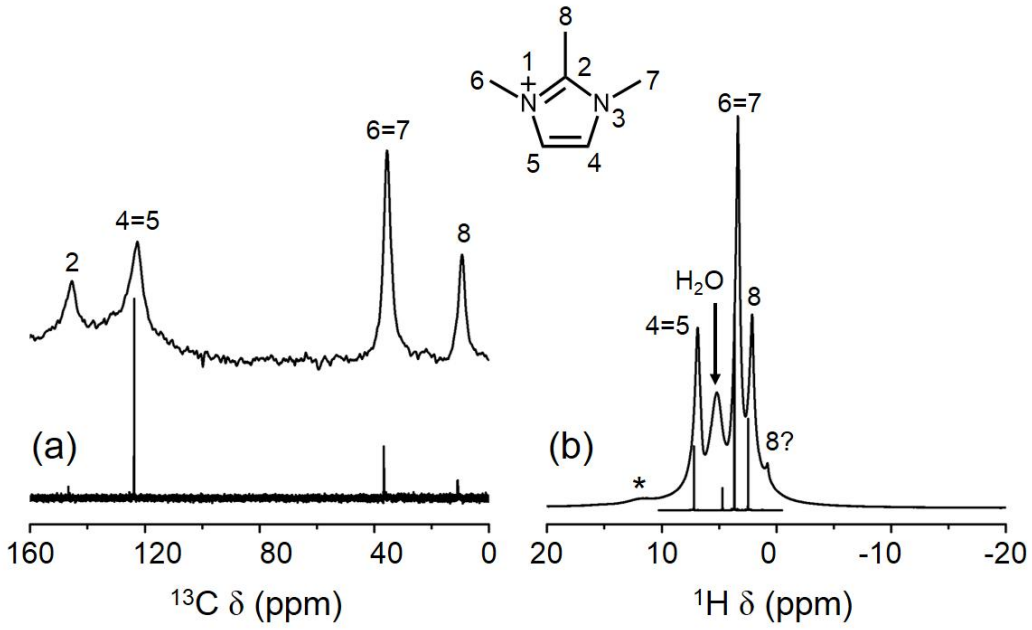

Figure 4: ^{1}H–^{13}C CP (left) and ^{1}H (right) MAS NMR spectra of as–made HPM-5 (top traces) and ^{13}C and ^{1}H NMR spectra of the pristine 123TMI^{+} cation in D_2O solution (bottom, left and right, respectively). The resonance at 11.6 ppm, characteristic of the protons in hydrogen bonded SiOH defects is marked with an asterisk.[16,17]

signed), another quite strong around 5.2 ppm assigned to the protons in OH groups or H_2O molecules involved in weak hydrogen bonding, and a weak and broad resonance around 11.6 ppm characteristic of significantly deshielded protons in silanol groups involved in relatively strong hydrogen bonds with an oxygen to oxygen distance (O–H$\cdots$ O) of around 2.64 Å.[18] These hydrogen bonds are slightly stronger than those typically found in defects in pure and high silica zeolites synthesized in basic media (characterized by a ^{1}H resonance around 10.2 ppm and an O–H$\cdots$ O distance around 2.70 Å)[16] and quite weaker than the typical inter-layer hydrogen bonds typically found in layered zeolite precursors and other layered silicates (resonance around 16 ppm, or an O–H$\cdots$ O distance of 2.45 Å distance).[17,19–25]

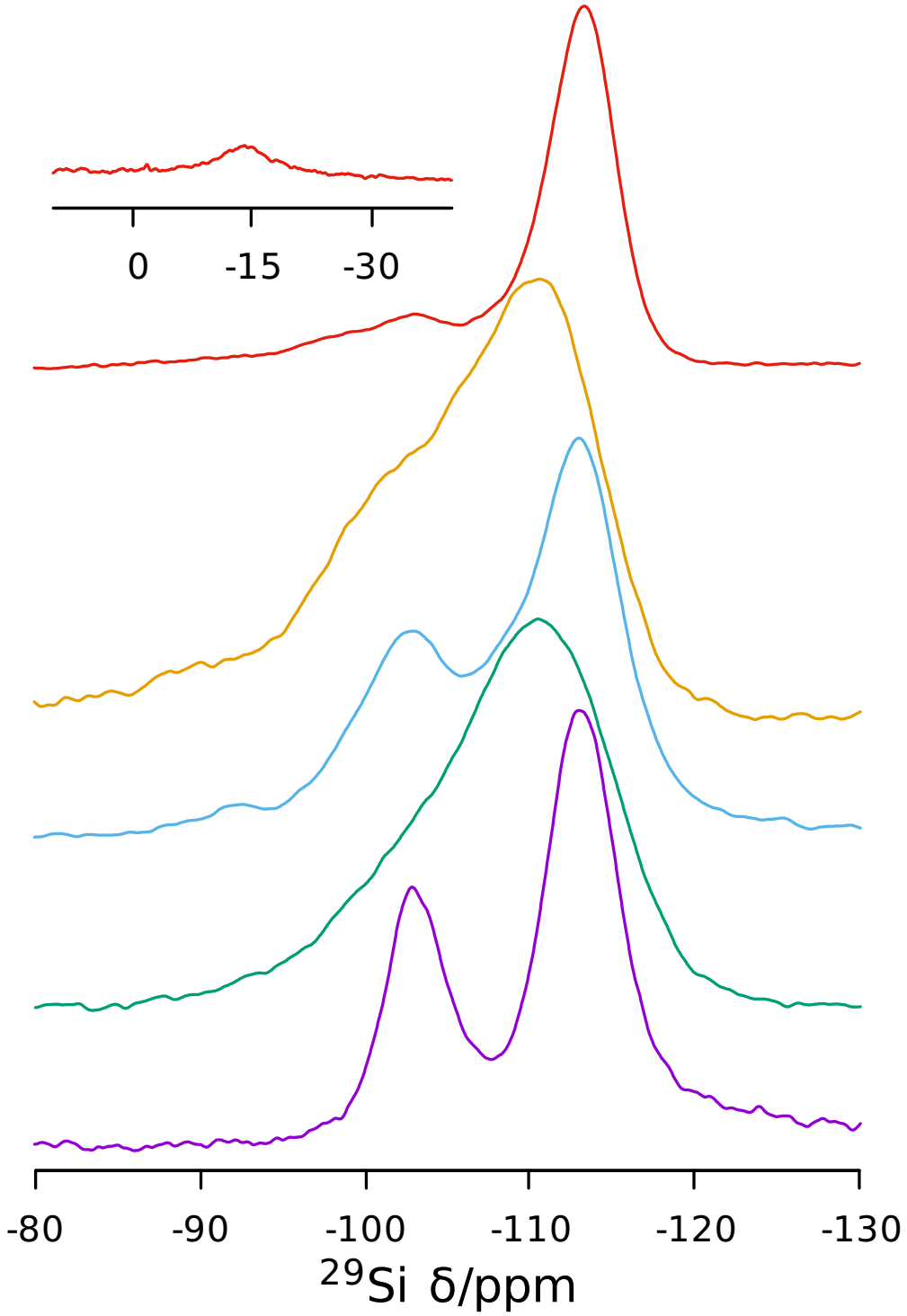

Figure 5: ^{29}Si MAS NMR spectra of (from bottom to top) as–made and calcined HPM-5, delaminated, 'delaminated' and calcined and silylated derivatives of HPM-5. The inset shows the resonance assigned to –O–Si$(CH_3)_2$–O– units in the silylated material.

The existence of a high concentration of Si-O^- connectivity defects, evidenced in the IR and ^{1}H NMR spectra, is further supported by ^{29}Si MAS NMR spectroscopy (Fig. 5, right). The spectrum presents two relatively sharp resonances, one around -103 ppm that may be assigned to Q_3 defects (i.e. $\underline{\text{Si}}(\text{OSi})_3\text{O-}$) or to Q_4 $\underline{\text{Si}}(\text{OSi})_3\text{OAl}$, and another one at -113 ppm, assigned to siliceous Q_4 sites (i.e. $\underline{\text{Si}}(\text{OSi})_4$). However, these two resonances are in an intensity ratio of ca. 1 : 2, respectively, implying that the contribution of connectivity defects to the -103 ppm must be dominant: the Si/Al ratio of this zeolite is rather high (30) compared to the value that would be derived by assuming that the -103 ppm resonance is mainly due to $\underline{\text{Si}}(\text{OSi})_3\text{OAl}$ species (calculated Si/Al ca. 10). Upon calcination the spectrum shows a single, very broad and asymmetric resonance around -111 ppm, which should correspond to the overlapped $\underline{\text{Si}}(\text{OSi})_4$, $\underline{\text{Si}}(\text{OSi})_3\text{O})^-$, and $\underline{\text{Si}}(\text{OSi})_3\text{OAl}$ resonances.

The incorporation of Al into the material is confirmed by ^{27}Al MAS NMR, which shows a clear resonance around -50 ppm, assigned to tetrahedral $\underline{\text{Al}}(\text{OSi})_4$ in the zeolite framework (Supporting Information Fig. S3). However, the spectrum of the calcined sample shows also a prominent and broad resonance around 0 ppm, characteristic of octahedral Al, suggesting a much significant extraction of framework Al upon calcination.

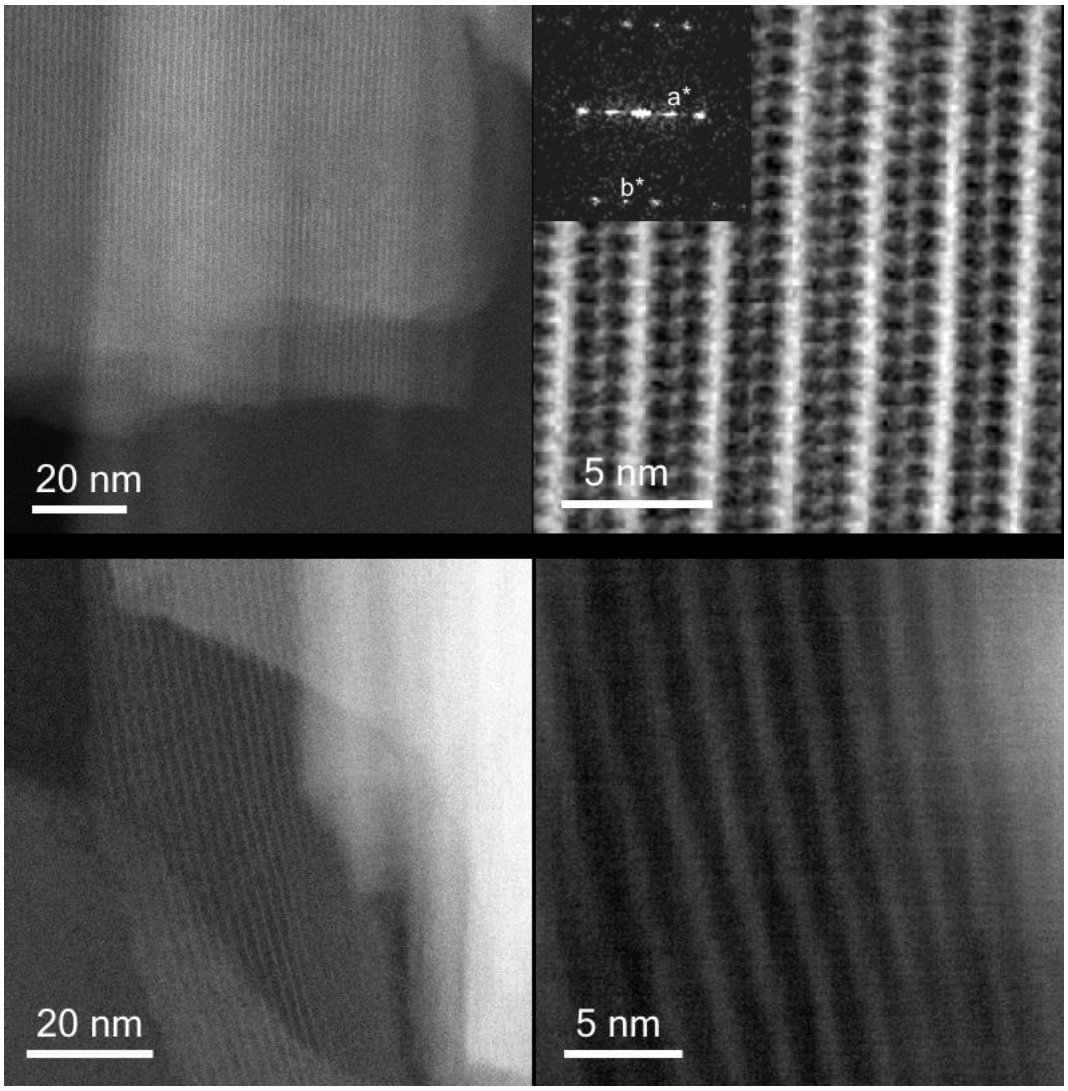

Figure 6: C_s-corrected STEM-HAADF analysis of the of as-made (top) and calcined HPM-5 (bottom). Low-magnification images are shown in the left part. High-resolution image of the as-made HPM-5 (top right) presenting the nature of the inter-layers with its corresponding FFT (inset). Right bottom corresponds to the closest observation of the calcined HPM-5 material.

The very broad and heavily overlapped reflections of HPM-5 hinders its structural elucidation by XRD analysis, for both the as–made and calcined materials. Thus, we have attempted to extract more information by TEM; despite the difficulties of applying TEM to microporous solids, very interesting data have been produced in the recent years through C_s-corrected STEM using a high angle annular dark field (HAADF) detector,[26,27] although the very thin domains of HPM-5 prevented an extensive investigation along different ori-

entations. As shown in Fig. 6 left, both as–made and calcined materials appear to have a layered structure. However, a closer inspection at higher magnification of the as–made material also shows that dense areas spaced by around 2 nm are connected by less dense material conforming a regular and intricate array of pores and yielding a lace–like appearance, Fig. 6, top right. The FFT shown in the inset reveals two lattice distances that correspond to a* $\approx$ 20.24 Å (representing the layer spacing) and a shorter distance d* $\approx$ 6.96 Å that may be associated with the intralayer structure. We were not able to reach the same resolution in the calcined material, where only 'layers' with similar d-spacings, around 2nm, were observed, Fig. 6, bottom.

Derived materials

The abundance of Q_3 Si sites in HPM-5 could be a result of not only its small, nanosized structural domains (Fig. 3) but also of a layered nature of the material (Fig. 6). If this were the case, the rich intralayer chemistry characteristic of layered silicates and zeolite precursors could be applied to it.[28–32] In fact, calcination produces large changes in the powder XRD pattern and its failure in producing a highly crystalline material may be due to a number of reasons, including turbostratic disorder[33] and, more simply, an inadequate disposition of silanol groups in adjacent layers.

We first tried the delamination of as–made HPM-5 by the procedure described in the experimental section. The XRD pattern shows only two peaks around 25.0 and 26.1° (already presented in the as–made material, Fig. 7. After calcination at 550 °C these peaks are no longer visible, but two peaks at 12.5 and 12.9° have developed. The as–made sample also shows a broad peak at similar angles, which may also be present with very little intensity in the 'delaminated' uncalcined sample.

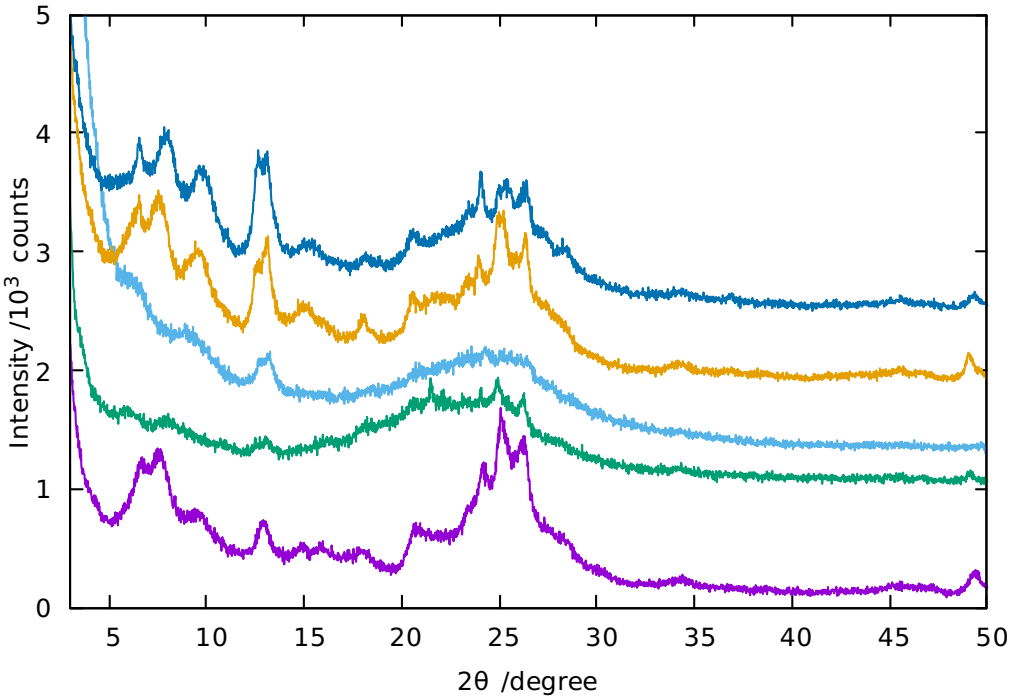

Figure 7: Powder XRD patterns of (from bottom to top): as–made, delaminated, 'delaminated' and calcined, silylated and silylated and calcined forms of HPM-5.

Fig. 5 shows the ^{29}Si MAS NMR spectra of 'delaminated' HPM-5 before and after calcination. After delamination, the two resonances appearing at -103 and -113 ppm in the spectrum of as–made HPM-5 are still present, but significantly broadened. Additionally, there is a small and broad resonance at -92 ppm, which we assign to Q_2 defect sites (i.e. to $\underline{\text{Si}}(\text{OSi})_2\text{O}_2{}^{2-}$) and which was not evident in the spectrum of the as–made material. After calcination at 550 °C), the resonances are also broader than for calcined HPM-5 (see Fig. 5), the Q_3 band increases in intensity and the presence of Q_2 defect sites is also noticeable. This evidences a significant increase in the concentration of connectivity defects by the delamination process, revealing a decreased connectivity after the delamination reaction, which can be further supported by IR spectroscopy. As show in Fig. 8, the vibrations around 960 cm^{-1} increase in relative intensity but also develop as two sharper bands at 962 and 910 cm^{-1}. After calcination, however, there is a broader and intense band at 960 with possibly a broad shoulder around 905 cm^{-1}.

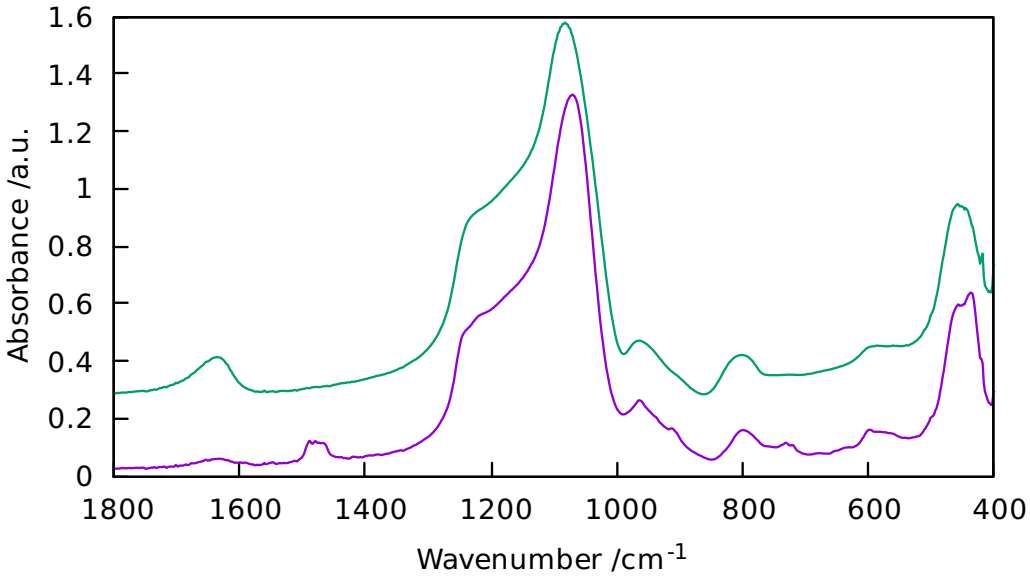

Figure 8: IR spectra of materials derived from HPM-5: 'delaminated' (bottom), and 'delaminated' and calcined (top).

The N_2 BET surface area of calcined 'delaminated' HPM-5 was determined to be 630 $m^2 g^{-1}$, with essentially no microporosity. This surface area is much higher than that of calcined HPM-5 (around 200 $m^2 g^{-1}$). There is also almost no hysteresis loop in the N_2 adsorption-desorption isotherms, Supporting Infomation Fig. S4. This implies that, if the material resulting from the delamination reaction is truly a delaminated derivative, the layers are not arranged through edge-to-face orientation, unlike the case of ITQ–2.[29]

The electron microscopy images of 'delaminated' HPM-5 in Figure 9, shows that, in addition to unstructured material, there are features that present evident porosity reminiscent of those found in the upper right TEM image of Figure 6, but with a much decreased size in one dimension, resembling 1D zig-zag ribbons rather than 2D layers. The pore opening determined from the left TEM image in Figure 9 would be around 16.7 Å.

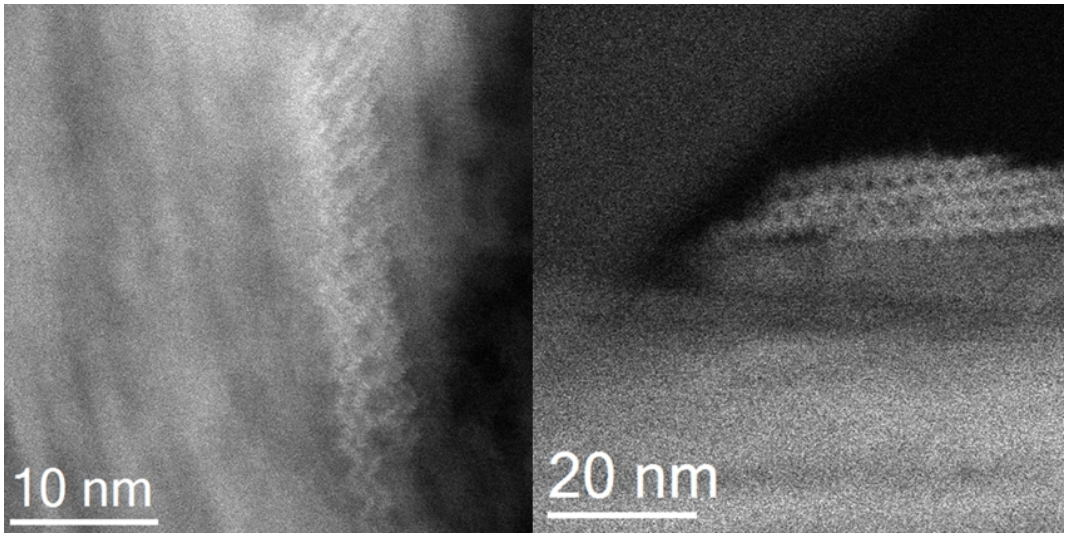

Figure 9: C_s-corrected STEM-HAADF analysis of HPM-5 after 'delamination' reaction.

Next, we attempted the interlayer expansion reaction to produce an IEZ-like material,[31] by following the procedure described in the experimental section to an as–made HPM-5 material. As shown in Fig. 7, the reaction produces just a minor shift of the first reflection by about 0.3° to lower angles (corresponding to an expansion of less than 0.1 Å), with no further changes upon calcination (contrarily to the changes observed upon calcination of the untreated material). A new reflection around 12.7° is also observed in the silylated samples before and after calcination.

The ^{29}Si MAS NMR spectrum of the silylated sample in Fig. 5 gives a resonance at -14.6 ppm typical of tetrahedral Si bonded to two carbon and two oxygen atoms. This clearly reveals the successful introduction of –O–Si$(CH_3)_2$–O– units.[12,34] Compared to the spectrum of as–made HPM-5, in addition, the relative intensity of the peak assigned to Q_3 species is weaker, further confirming the successful silylation. From the analysis of the N_2 isotherms, Supporting Information Fig. S5, the BET and external surface areas of the silylated, calcined HPM-5 material were determined to be 295 and 125 m^2g^{-1}, respectively, higher values than those of calcined HPM-5. The micropore volume after the treatment (0.08 cm^3g^{-1}) is similar to the values observed for calcined HPM-5. However, the STEM images of the silylated sample in Figure 10 shows mostly unstructured material together with

ribbons similar to those found in Figure 9. In this case, the ribbons, which are undulated, contain windows that closely resemble those observed in the as-made material (Figure 6, upper right). The pore size measured in this case is similar to that observed in Figure 9, giving a value of approximately 15 Å (Figure 10, bottom right). The difficulties associated with a low beam stability, as well as with the particular morphology of the sample, have not allowed to reach atomic resolution in order to clearly discern the number of members making the rings (MR); however, from the large pore openings observed in Figures 9 and 10 we deem likely that 14 MR are present in the structure. These results might suggest that HPM-5 posses tiny layers containing a high density of large or extralarge pores, rendering it not as stable as to be able to produce 'delaminated' and interlayer expanded derivatives by the conventional reactions. Rather, deconstruction of the material apparently occurs, and the layers brake into ribbons (some of which maintain the inner windows) and unstructured material.

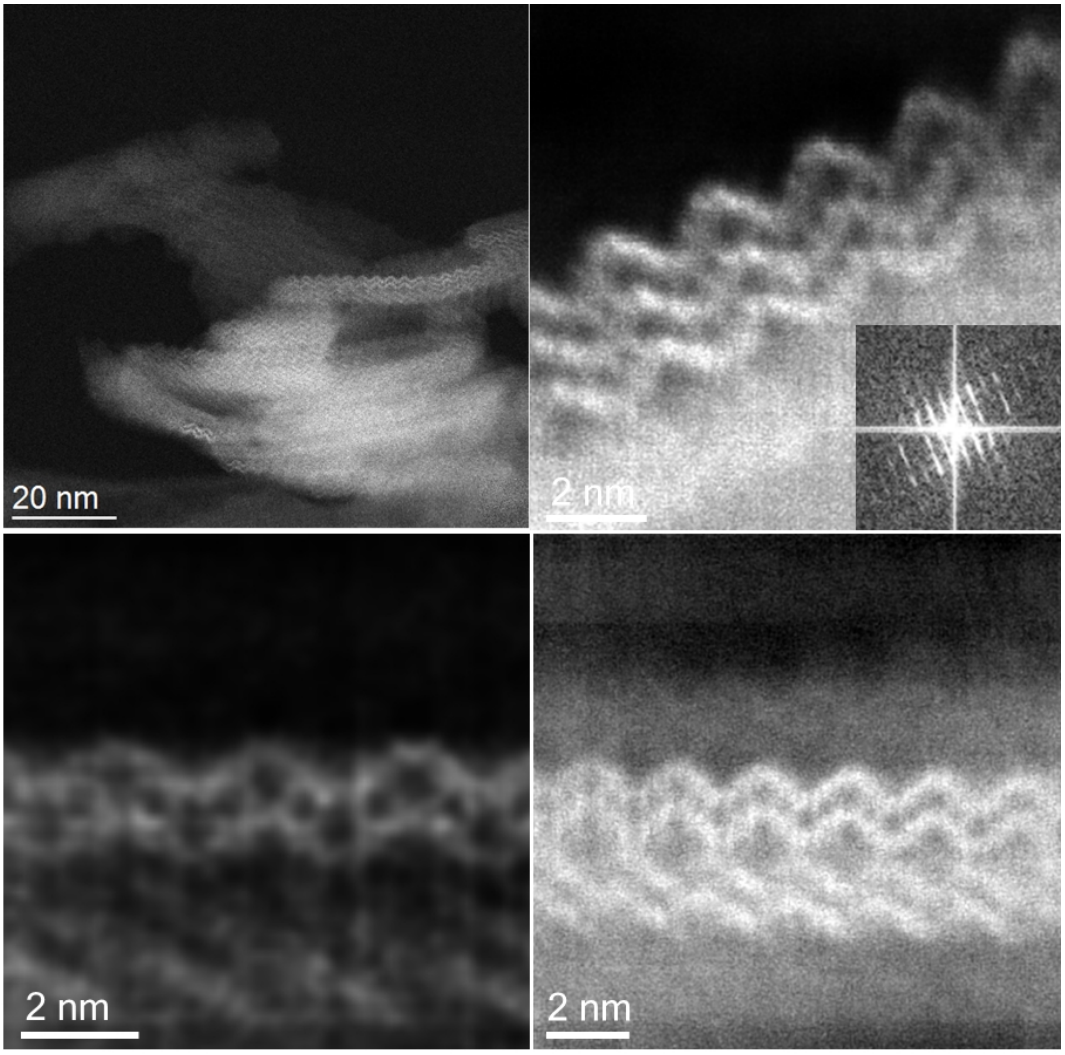

Figure 10: C_s-corrected STEM-HAADF analysis of HPM-5 after the silylation reaction.

Conclusions

HPM-5 is a new (alumino)silicate material synthesized under a wide range of conditions using 1,2,3-trimethylimidazolium in hydroxide media and displays a delicate flower-like morphology. As intended, the deliberate absence of fluoride anions frustrates the ability of this organic cation to crystallize zeolite ITW, making possible instead the crystallization of HPM-5 (or RTH under a much narrower range of conditions, specifically requiring a much higher Al content).[10] HPM-5 is consistently characterized by its XRD pattern, despite show-

ing only broad and overlapped reflections. ^{29}Si MAS NMR and IR spectroscopies evidence the presence of a large concentration of connectivity defects and ^{1}H MAS NMR data show rather deshielded protons assigned to silanol groups involved in relatively strong hydrogen bonds. While C_s–corrected STEM generally reveals the existence of a porous layered-like structure in both the as–made and calcined forms of HPM-5, the higher resolution images obtained for the as–made material reveal a considerable structural intricacy. Calcination produces a porous material whose powder XRD pattern is still ill-defined. Nonetheless, when the as–made material is subjected to typical delamination and silylation procedures, the surface area increases in both cases. However, STEM reveals these derived materials are predominantly unstructured, while some ribbon-like features are also apparent. We conclude that HPM-5 may be formed by porous layers that are too unstable to afford delamination or interlayer expansion and are prone to disassembly into porous ribbons and amorphous material.

Acknowledgements

The authors acknowledge financial support from the Spanish Ministery of Science and Competitiveness (Projects MAT2012-31759 and MAT2015-71117-R) and from the National Creative Research Initiative Program (2012R1A3A2048833) through the National Research Foundation of Korea. We also thank A. Valera for technical help (FESEM and EDS). A. M. acknowledges European Union Seventh Framework Programme under Grant Agreement No. 312483–ESTEEM2 (Integrated Infrastructure Initiative–I).

Supporting Information

Thermogravimetric and differential thermal traces for as–made HPM-5, ^{27}Al MAS NMR spectra of as–made and calcined HPM-5, N_2 adsorption-desorption isotherms of calcined HPM-5 and of the calcined forms of its 'delaminated' and silylated derivatives.

References

(1) Davis, M. E.; Lobo, R. F. *Chem. Mater.* **1992**, *4*, 756–768.

(2) Guth, J. L.; Kessler, H.; Caullet, P.; Hazm, J.; Merrouche, A.; Patarin, J. In *Proceedings of 9th International Zeolite Conference*; von Ballmoos, R., Higgins, J., Treacy, M., Eds.; Butterworth-Heinemann, 1993; pp 215–222.

(3) Caullet, P.; Paillaud, J. L.; Simon-Masseron, A.; Soulard, M.; Patarin, J. *C. R. Chim.* **2005**, *8*, 245–266.

(4) Zicovich-Wilson, C. M.; San-Roman, M. L.; Camblor, M. A.; Pascale, F.; Durand-Niconoff, J. S. *J. Am. Chem. Soc.* **2007**, *129*, 11512–11523.

(5) Rojas, A.; Luisa San-Roman, M.; Zicovich-Wilson, C. M.; Camblor, M. A. *Chem. Mater.* **2013**, *25*, 729–738.

(6) Barrett, P. A.; Boix, T.; Puche, M.; Olson, D. H.; Jordan, E.; Koller, H.; Camblor, M. A. *Chem. Commun.* **2003**, 2114–2115.

(7) Yang, X.; Camblor, M. A.; Lee, Y.; Liu, H.; Olson, D. H. *J. Am. Chem. Soc.* **2004**, *126*, 10403–10409.

(8) Rojas, A.; Martinez-Morales, E.; Zicovich-Wilson, C. M.; Camblor, M. A. *J. Am. Chem. Soc.* **2012**, *134*, 2255–2263.

(9) Rojas, A.; Camblor, M. A. *Dalton Trans.* **2014**, *43*, 10760–10766.

(10) Jo, D.; Lim, J. B.; Ryu, T.; Nam, I.-S.; Camblor, M. A.; Hong, S. B. *J. Mater. Chem. A* **2015**, *3*, 19322–19329.

(11) Jung, H. J.; Park, S. S.; Shin, C.-H.; Park, Y.-K.; Hong, S. B. *J. Catal.* **2007**, *245*, 65–74.

(12) Gies, H.; Müller, U.; Yilmaz, B.; Feyen, M.; Tatsumi, T.; Imai, H.; Zhang, H.; Xie, B.; Xiao, F.-S.; Bao, X.; Zhang, W.; Baerdemaeker, T. D.; De Vos, D. *Chem. Mater.* **2012**, *24*, 1536–1545.

(13) Rojas Nuñez, A. E. 'Dirección de Estructuras en la Síntesis de Zeolitas Usando Cationes Orgánicos Imidazolios'. Ph.D. thesis, Universidad Autónoma de Madrid, 2012.

(14) Barrett, P. A.; Díaz-Cabañas, M. J.; Camblor, M. A. *Chem. Mater.* **1999**, *11*, 2919–2927.

(15) Camblor, M. A.; Corma, A.; Valencia, S. *Microporous Mesoporous Mater.* **1998**, *25*, 59–74.

(16) Koller, H.; Lobo, R. F.; Burkett, S. L.; Davis, M. E. *J. Phys. Chem.* **1995**, *99*, 12588–12596.

(17) Apperley, D.; Hudson, M.; Keene, M.; Knowles, J. *J. Mater. Chem.* **1995**, *5*, 577–582.

(18) Eckert, H.; Yesinowski, J.; Silver, L.; Stolper, E. *J. Phys. Chem.* **1988**, *92*, 2055–2064.

(19) Burton, A.; Accardi, R.; Lobo, R.; Falcioni, M.; Deem, M. *Chem. Mater.* **2000**, *12*, 2936–2942.

(20) Borowski, M.; Marler, B.; Gies, H. *Z. Kristallogr.* **2002**, *217*, 233–241.

(21) Wang, Y. X.; Gies, H.; Marler, B.; Müller, U. *Chem. Mater.* **2005**, *17*, 43–49.

(22) Wang, Y. X.; Gies, H.; Lin, J. H. *Chem. Mater.* **2007**, *19*, 4181–4188.

(23) Gies, H.; Marler, B. *Acta Crystallogr.* **2011**, *A67*, C651–C652.

(24) Marler, B.; Li, Z.; Wang, G.; Gies, H. *Acta Crystallogr.* **2011**, *A67*, C650.

(25) Marler, B.; Grünewald-Lüke, A.; Grabowski, S.; Gies, H. *Z. Kristallogr.* **2012**, *227*, 427–437.

(26) Mayoral, A.; Carey, T.; Anderson, P. A.; Diaz, I. *Microporous Mesoporous Mater.* **2013**, *166*, 117–122.

(27) Mayoral, A.; Min, J. G.; Hong, S. B. *Microporous Mesoporous Mater.* **2016**, *236*, 129–133.

(28) Roth, W. J.; Kresge, C. T.; Vartuli, J. C.; Leonowicz, M. E.; Fung, A. S.; McCullen, S. B. *Stud. Surf. Sci. Catal.* **1995**, *94*, 301–308.

(29) Corma, A.; Fornes, V.; Pergher, S.; Maesen, T.; Buglass, J. *Nature* **1998**, *396*, 353–356.

(30) Fan, W.; Wu, P.; Namba, S.; Tatsumi, T. *Angew. Chem. Int. Ed.* **2004**, *43*, 236–240.

(31) Inagaki, S.; Yokoi, T.; Kubota, Y.; Tatsumi, T. *Chem. Commun.* **2007**, 5188–5190.

(32) Wu, P.; Ruan, J.; Wang, L.; Wu, L.; Wang, Y.; Liu, Y.; Fan, W.; He, M.; Terasaki, O.; Tatsumi, T. *J. Am. Chem. Soc.* **2008**, *130*, 8178–8187.

(33) Roth, W. J.; Dorset, D. L.; Kennedy, G. J. *Microporous Mesoporous Mater.* **2011**, *142*, 168–177.

(34) Ruan, J.; Wu, P.; Slater, B.; Zhao, Z.; Wu, L.; Terasaki, O. *Chem. Mater.* **2009**, *21*, 2904–2911.

Table of Contents Entry

The new microporous material HPM-5 has an intricate structure composed of lace–like layers that are too labile to withstand delamination or intelayer expansion.